Available online at www.sciencedirect.com
ScienceDirect
Cement and Concrete Research 37 (2007) 1152–1163
Cement and Concrete Research

Comparative study of methods used to estimate ionic diffusion coefficients using migration tests

G.A. Narsilio [a], R. Li [a,b], P. Pivonka [a], D.W. Smith [a,*]

[a] Department of Civil and Environmental Engineering, School of Engineering, The University of Melbourne, Victoria 3010, Australia
[b] Institute of Geotechnical Engineering, Southeast University (SEU), Nanjing, Jiangsu, China

Received 23 August 2006; accepted 23 May 2007

Abstract

Ionic diffusion coefficients are estimated rapidly using electromigration tests. In this paper, electromigration tests are accurately simulated by numerically solving the Nernst–Planck (NP) equation (coupled with the electroneutrality condition (EN)) using the finite element method. Numerical simulations are validated against experimental data obtained elsewhere [E. Samson, J. Marchand, K.A. Snyder, Calculation of ionic diffusion coefficients on the basis of migration test results, Materials and Structures/Matériaux et Constructions 36 (257) (2003) 156–165., H. Friedmann, O. Amiri, A. Aït-Mokhtar, A direct method for determining chloride diffusion coefficient by using migration test, Cement and Concrete Research 34 (11) (2004) 1967–1973.]. It is shown that migration due to the non-linear electric potential completely overwhelms diffusion due to concentration gradients. The effects of different applied voltage differences and chloride source concentrations on estimations of chloride diffusion coefficients are explored. We show that the pore fluid within concrete and mortar specimens generally differs from the curing solution, lowering the apparent diffusion coefficient, primarily due to interactions of chloride ions with other ions in the pore fluid. We show that the variation of source chloride concentration strongly affects the estimation of diffusion coefficients in non-steady-state tests; however this effect vanishes under steady-state conditions. Most importantly, a comparison of diffusion coefficients obtained from sophisticated analyses (i.e., NP–EN) and a variety of commonly used simplifying methods to estimate chloride diffusion coefficients allows us to identify those methods and experimental conditions where both approaches deliver good estimates for chloride diffusion coefficients. Finally, we demonstrate why simultaneous use and monitoring of current density and fluxes are recommended for both the non-steady and steady-state migration tests.

Keywords: Multi-ion transport; Migration tests; Nernst–Planck equation; Electroneutrality; Apparent chloride diffusion coefficient; Concrete durability

1. Introduction

The estimation of concrete durability has become increasingly important for both durability modeling and the maintenance planning for civil engineering structures. Steel corrosion significantly impacts on the service life of reinforced concrete structures. Marine environments and deicing salts on bridges prompt chloride transport from the concrete surfaces towards the reinforcing steel [3]. Chloride ions accelerate steel corrosion by depassivation processes and so the service life of reinforced concrete structures is reduced. Chloride transport through concrete results from: 1) advective transport within the concrete micropores due to pore-water pressure gradients, 2) diffusive transport due to chloride concentration gradients [4,5]. The second mechanism dominates in the absence of pressure gradients in completely saturated concretes [6]. The accurate experimental determination of diffusion coefficients is crucial for estimating the service life of reinforced concrete [7]. Herein, we focus on the estimation of effective chloride diffusion coefficient using electromigration tests. There are several variations of this test and a variety of different methods are used to calculate ion diffusion coefficients. The employed methods generally differ in the simplifying assumptions. As a result there is a rather large variability in reported diffusion coefficients

* Corresponding author. Tel.: +61 3 8344 4050; fax: +61 3 8344 4616.
E-mail addresses: narsilio@unimelb.edu.au (G.A. Narsilio), lirenmin@seu.edu.cn (R. Li), ppivonka@unimelb.edu.au (P. Pivonka), david.smith@unimelb.edu.au (D.W. Smith).
URL: http://www.civenv.unimelb.edu.au (D.W. Smith).

0008-8846/$ - see front matter © 2007 Elsevier Ltd. All rights reserved.
doi:10.1016/j.cemconres.2007.05.008

obtained from migration test compared with those from more traditional diffusion tests [8–10]. A number of factors have been postulated to contribute to these discrepancies such as temperature, intensity of applied electric field, electrode types, chemical activity and composition and concentration of the testing solution [1,10–13]. The primary aims of the paper are to investigate and resolve some of the above mentioned discrepancies for migration tests. For this purpose we perform state-of-the-art numerical simulations of migration experiments using a sophisticated multi-ion transport model, i.e., the Nernst–Planck equation coupled with the electroneutrality condition. This model allows us to numerically simulate migration tests and to improve the fundamental physical understanding of ion migration in concrete and mortar and its relationship to the estimation of diffusion coefficients. The experimental conditions and methods that lead to good estimates of chloride diffusion coefficients are revealed by comparing the diffusion coefficients that are obtained on the basis of the Nernst–Planck equation coupled to the electroneutrality condition and the estimates obtained from a variety of commonly employed simplified methods. Finally, experimental test design optimization and suitable test protocols are outlined.

2. Ion transport governing equations

The general equation describing ion electrodiffusive transport at the macroscale is the generalized Nernst–Planck equation [14]. The average ionic flux density j_i through saturated uncharged specimens in one dimension is given by,

$$j_i = -(\tau\cdot\varphi\cdot D_{0i})\left(\frac{\partial c_i}{\partial x}+\frac{z_i\cdot F}{R\cdot T}c_i\frac{\partial\psi}{\partial x}+c_i\frac{\partial \ln\gamma_i}{\partial x}-\frac{c_i\cdot V_x}{(\tau\cdot\varphi\cdot D_{0i})}\right) \quad (1)$$

where τ is the tortuosity of the cement-based specimen (i.e., concrete or mortar); φ is its porosity; D_{0i} is the self-diffusion coefficient of ion i; c_i is the average concentration of the ith ion in the fluid phase; z_i is the ith ion charge; F=96,485.3 C mol^{-1} is the Faraday constant; R=8.3144 J mol$^{-1}\cdot$K^{-1} is the universal gas constant; T is the absolute temperature; ψ is the voltage; γ_i is the chemical activity coefficient; and V_x is the average velocity of the fluid.

We shall use Eq. (1) as the fundamental equation describing the behaviour of electromigration tests. These tests are performed on saturated specimens. Moreover, the advection term in Eq. (1) can be ignored as no pressure gradients are applied or generated during testing. On the other hand, chemical reactions can be neglected in most migration tests since the application of an electric field produces an ionic transport rate much faster than the kinetics of chemical reactions in concrete. By the separation of time scales the influence of the chemical reactions on the overall transport is minimized [1,15,16]. Furthermore, it has been shown that one can also neglect the chemical activity term in non-steady-state migration tests [1,17].

The tortuosity τ in Eq. (1) is the result of volume averaging the microscopic Nernst–Planck equation. It is a geometrical quantity that measures the tortuosity of the pathways followed by the diffusing ions as a result of the pore space morphology. The values of τ range from 0 (impervious pores) to 1 (free water) [1,18]. The tortuosity τ and the porosity φ are intrinsic characteristic of the material and must be constant for uncharged porous materials like concrete in the absence of chemical reactions. In this case it is possible to define an apparent ion diffusion coefficient[1] [18,19]

$$D_i = \varphi\cdot\tau\cdot D_{0i} \quad (2)$$

Given these assumptions for migration tests and recalling Eq. (2), the one-dimensional average ionic flux j_i in Eq. (1) can be simplified to,

$$j_i = -D_i\left(\frac{\partial c_i}{\partial x}+\frac{z_i\cdot F}{R\cdot T}c_i\frac{\partial\psi}{\partial x}\right) \quad (3)$$

where D_i is the apparent diffusion coefficient of ion i; c_i is the average fluid concentration of the ith ion; z_i is the ith ion charge; F, R and T are the Faraday constant, gas constant, and absolute temperature; and ψ is the electrical potential. Eq. (3) implies that the unidirectional ith ionic flux is constituted by a diffusion plus a migration component [6]. The electrical current density i_{elec} passing through a specimen is a function of the flux j_i given by Eq. (3),

$$i_{\text{elec}} = F\cdot\sum_{i=1}^{N} z_i\cdot j_i \quad (4)$$

where N denotes the total number of ions present in the pore solution.

Mass conservation for each ion species is expressed as

$$\varphi\frac{\partial c_i}{\partial t} = -\frac{\partial j_i}{\partial x} \quad (5)$$

and so the macroscopic governing equation for ionic transport (where the influence of chemical reactions on the overall mass transport has been neglected) leads to,

$$\varphi\frac{\partial c_i}{\partial t}-\frac{\partial}{\partial x}\left[D_i\left(\frac{\partial c_i}{\partial x}+\frac{z_i\cdot F}{R\cdot T}c_i\frac{\partial\psi}{\partial x}\right)\right]=0 \quad (6)$$

where c_i is the average fluid concentration of the ith ion; t represents time; D_i is the apparent diffusion coefficient of ion i; z_i is the ith ion charge; F, R and T are the Faraday constant, gas constant, and absolute temperature; and ψ is the voltage.

The system of Eq. (6) must be solved simultaneously with another equation that couples the transport of all ionic species, viz, the electroneutrality condition [20]:

$$\sum_{i=1}^{N} z_i\cdot c_i = 0 \quad (7)$$

[1] Eq. (2) must not be confused neither with the Fick's second law fitting parameter D^{app} such that $\partial c/\partial t=-D^{\text{app}}\partial^2 c/\partial x^2$ nor with the effective diffusion coefficient $D^{\text{eff}}=\tau\cdot D_{0i}$.

where N is the total number of ionic species in the system. Eq. (7) holds in all solutions at the macroscale for uncharged porous materials, except very close to the electrodes in migration tests [21,22].

In steady-state conditions, the flux is constant and the time dependent term in Eq. (6) vanishes. Moreover, it is usually assumed that the 'diffusion component' of the transport is overwhelmed by the 'migration component' of the transport due to the relatively large applied external voltage. Many researchers also choose to assume a constant field [2,6,7,10], even though the constant field assumption tends to overestimate the computed apparent diffusion coefficients D_i [1,23].

We quantify deviations arising from simplifying assumptions as a function of the applied external voltage and salt concentrations, and by this means, we provide further insight into modeling, design and interpretation of migration tests.

3. Migration tests

The classical two compartments cell experimental setup has been historically used to estimate diffusion coefficients. In general, one of the cells acts as a source containing a chloride solution while the other holds a chloride-free solution. The chloride flux passing through the cement-based specimen between the two cells is computed from the measured time-varying chloride ionic concentrations in both chambers. These diffusion tests are usually time consuming (in the order of months or even years).

Alternatively accelerated tests protocols have been proposed over the last decades. Application of an external electrical potential has been found to drive ions through specimens considerably faster. Using this approach, the estimation of diffusion coefficients is accelerated and the respective tests are now known as electromigration (or more simply as migration) tests [1,2,7,10,12,23]. There are several variations of migration tests. Fig. 1 shows a schematic representation of a typical experimental setup. Samples are prepared and cured while saturated in an alkaline solution, usually sodium hydroxide (NaOH) and/or potassium hydroxide (KOH) solutions, and sectioned into specimens with thicknesses (l) ranging from

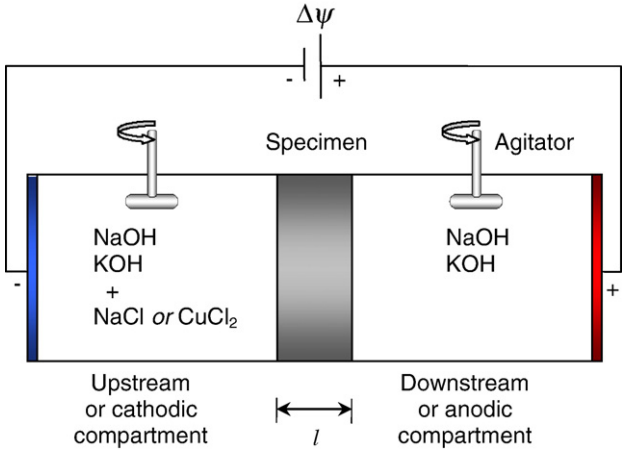

Fig. 1. Migration tests: schematic representation of a typical experimental setup.

Table 1
Values of ξ as a function of the bulk concentration

c_0 [mol/m^3]	ξ	$c_{i\ U,0}$ and $c_{i\ U,BC}$ [mol/m^3]		
		Na^+	Cl^-	OH^-
12		312	12	300
125	−0.107	425	125	300
250	0.412	550	250	300
500	0.764	800	500	300
750	0.934	1050	750	300
1000	1.044	1300	1000	300
1500	1.187	1200	1500	300

Notation: c_0 — initial concentration; $\xi = \mathrm{erf}^{-1}[1-(2\cdot c_d/c_0)]$; erf — error function and $c_d \approx 0.07$; $c_{i\ U,0}$ — upstream initial concentrations (at time $t=0$); $c_{i\ U,BC}$ — upstream concentration boundary condition.

25 mm for mortars to 50 mm for concrete. Subsequently, specimens are placed in the experimental device. Initially, the upstream or cathodic compartment and the downstream or anodic compartment contain a solution identical to the curing solution so as to minimize leaching and to conserve the microstructure of the material to be tested [1,2]. Later, a salt such as sodium chloride (NaCl) or copper chloride ($CuCl_2$) is added to the upstream compartment at a predetermined concentration and an electrical field ranging from 400 to 1200 V m^{-1} is applied using electrodes of different type, such as steel or copper electrodes, depending on the added salt.

As for 'standard' diffusion tests, migrations experiments can be classified as steady-state and non-steady-state tests. During steady-state migration tests, the time-varying chloride ionic concentrations are measured in both compartments. On the other hand, the current passing through the specimen or the ion penetration within it is measured during non-steady-state migration tests. Accordingly, researchers propose different ways of calculating diffusion coefficients.

For example, the ith ionic flux j_i through a specimen of cross-section A_s is computed as a function of the molar increment of the ith ion n_i in the time interval Δt as [2,23]:

$$j_i = \frac{n_i}{A_s \cdot \Delta t} = \frac{\Delta c_i \cdot V_{\text{compartment}}}{A_s \cdot \Delta t} \tag{8}$$

In steady-state, j_i remains constant and the apparent diffusion coefficient D_i can be determined using the modified Nernst–Planck equation [1,2,6,7,10]:

$$D_i = \frac{R \cdot T}{F} \cdot \frac{j_i}{z_i \cdot \left(\frac{\Delta\psi}{l}\right) \cdot c_i} \tag{9}$$

where R, T and F are the gas constant, absolute temperature and Faraday constant, j_i is the ith ion molar flux density determined using Eq. (8), z_i is the ith ion charge, c_i is the concentration of the ith ion in the fluid phase, $\Delta\psi$ is the applied voltage difference, and l is the specimen thickness. Eq. (9) is widely used and is valid under the following assumptions: ionic mobilities in the upstream and downstream compartment solutions are several orders of magnitude higher than in the concrete and therefore only what happens inside the concrete

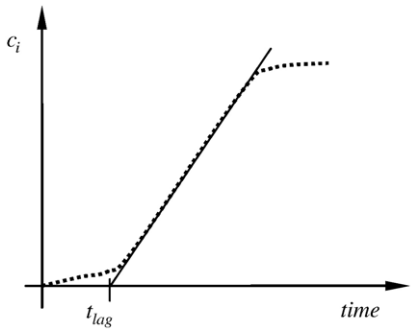

Fig. 2. Time-lag approach. Determination of t_{lag} (modified from [10]).

specimen is influencing the measurements; convection and chemical activity are neglected; the diffusive flux component in the Nernst–Planck equation is small in comparison to that due to migration and therefore is neglected; the specimen is thin and the steady-state is reached in few hours; the electrical potential varies linearly along the specimen; and the concentration (or activity) in the upstream compartment remains comparatively constant. So this expression arises from the application of simplifying assumptions to Eq. (3).

A more rigorous analytical solution can be expressed as [7]:

$$D_i = \frac{R\cdot T}{F}\cdot\frac{j_i}{z_i\cdot\left(\frac{\Delta\psi}{l}\right)}\cdot\frac{e^{z_iF\Delta\psi/RT}-1}{c_U\cdot e^{z_iF\Delta\psi/RT}-c_D} \tag{10}$$

where c_U and c_D represent the upstream and downstream ionic concentrations. Eq. (10) reduces to Eq. (9) when $e^{z_iF\Delta\psi/RT}>1$ and $c_U \geq c_D$.

The apparent diffusion coefficient D_i can be also estimated using the Nernst–Einstein equation since the flux j_i can be related to the current density i (Eq. (4)) through the transference number tr_i of the ionic species [6]:

$$D_i = \frac{R\cdot T}{F^2}\cdot\frac{i\cdot tr_i}{z_i\cdot\left(\frac{\Delta\psi}{l}\right)\cdot c_i} \tag{11}$$

In the case of migration tests using NaOH, KOH and NaCl, the chloride diffusion coefficient can also be computed as [2][2]

$$D_{Cl} = \frac{R\cdot T}{F^2}\cdot\frac{(i_0-i_f)}{\left(\frac{\Delta\psi}{l}\right)\cdot\left(\frac{c_{U(Cl)}}{c_{U(Cl)}+c_{U(OH)}}\cdot c_{U(OH)}\right)\cdot\left(\frac{D_{0OH}}{D_{0Cl}}-1\right)}\cdot\varphi \tag{12}$$

where i_0 and i_f are the initial and final measured current density upon the addition of NaCl, φ is the porosity, D_{0OH} and D_{0Cl} are the OH^- and Cl^- self-diffusion coefficients and c_U is the upstream ionic concentration. Eq. (12) also applies for migration test using NaOH and NaCl and it is based on the relationship given by Eq. (4), concentration balances during testing and after reaching steady-state within specimen and compartments, and flux conservation.

[2] We multiply the expression proposed by [2] times porosity to get the apparent diffusion coefficient as defined here in Eq. (2).

On the other hand, in non-steady-state migration tests, the diffusion coefficients are computed as [7,23]:

$$D_i = \frac{1}{a\cdot t}\cdot\left(\frac{2\cdot\xi^2}{a}+x_d-\frac{2\cdot\xi}{\sqrt{a}}\cdot\sqrt{\frac{\xi^2}{a}+x_d}\right) \tag{13}$$

where $a=z_i\cdot F\cdot\Delta\psi/(R\cdot T\cdot l)$; $\xi=\mathrm{erf}^{-1}[1-(2\cdot c_d/c_0)]$, erf is the error function and c_d is the ionic concentration at which the colour changes when using a colorimetric method to measure the penetration depth x_d, and c_0 is the initial concentration. The values of ξ as a function of c_0 for the common case of $c_d \approx 0.07$ M for chloride are given in Table 1. The application of Eq. (13) assumes that the electric field is large enough to produce some minimum chloride penetration at a given time t

Table 2
Summary of simplified formulae to estimate diffusion coefficients from migration tests

Steady-state tests	Equation	References
$D_i = \frac{R\cdot T}{F}\cdot\frac{j_i}{z_i\cdot(\Delta\psi/l)\cdot c_i}$	(9)	[1,2,6,7,10]
$D_i = \frac{R\cdot T}{F}\cdot\frac{j_i}{z_i\cdot(\Delta\psi/l)}\cdot\frac{e^{z_iF\Delta\psi/RT}-1}{c_U\cdot e^{z_iF\Delta\psi/RT}-c_D}$	(10)	[7]
$D_i = \frac{R\cdot T}{F^2}\cdot\frac{i\cdot tr_i}{z_i\cdot(\Delta\psi/l)\cdot c_i}$	(11)	[6]
$D_{Cl} = \frac{R\cdot T}{F^2}\cdot\frac{(i_0-i_f)\cdot\varphi}{(\Delta\psi/l)\cdot\left(\frac{c_{U(Cl)}}{c_{U(Cl)}+c_{U(OH)}}\cdot c_{U(OH)}\right)\cdot\left(\frac{D_{0OH}}{D_{0Cl}}-1\right)}$	(12)	[2]
Non-steady-state tests		
$D_i = \frac{1}{a\cdot t}\cdot\left(\frac{2\cdot\xi^2}{a}+x_d-\frac{2\cdot\xi}{\sqrt{a}}\cdot\sqrt{\frac{\xi^2}{a}+x_d}\right)$	(13)	[7,23]
$c_i = \frac{c_0}{2}\cdot\left[\mathrm{erfc}\left(\frac{x-a\cdot D_i\cdot t}{2\cdot\sqrt{D_i\cdot t}}\right)+e^{a\cdot x}\cdot\mathrm{erfc}\left(\frac{x+a\cdot D_i\cdot t}{2\cdot\sqrt{D_i\cdot t}}\right)\right]$	(14)	[1,7,23]
$D_i = \frac{2\cdot x_d^2\cdot\left(v\coth\frac{v}{2}-2\right)}{t_{lag}\cdot v^2}$	(15)	[10]

Notation: $j_i=n_i/(A_s\cdot\Delta t)$ — ith ion molar flux density, A_s — cross-section, n_i — molar increment of the ith ion in the time interval Δt; R, T and F — gas constant, absolute temperature and Faraday constant; z_i — ith ion charge; c_i — concentration of the ith ion in the fluid phase; ψ — voltage; l — specimen thickness; c_U and c_D — upstream and downstream ionic concentrations; i — current density; tr_i — transference number of the ionic species; i_0 — initial current density; i_f — final current density; φ — porosity; D_{0OH} — OH^- self-diffusion coefficient; D_{0Cl} — Cl^- self-diffusion coefficient; erfc — complementary error function; $a=z_i\cdot F\cdot\Delta\psi/(R\cdot T\cdot l)$; x_d — penetration depth; c_0 — initial concentration; $\xi=\mathrm{erf}^{-1}[1-(2\cdot c_d/c_0)]$; erf — error function, c_d — ionic concentration at x_d; $v=z_i\cdot q\cdot\Delta\psi/(k\cdot T)$, $k=1.380\ 6505\times10^{-23}$ J K^{-1} — Boltzmann's constant, $q=1.602\ 176\ 53\times10^{-19}$ C — elementary charge; and t_{lag} — time lag.

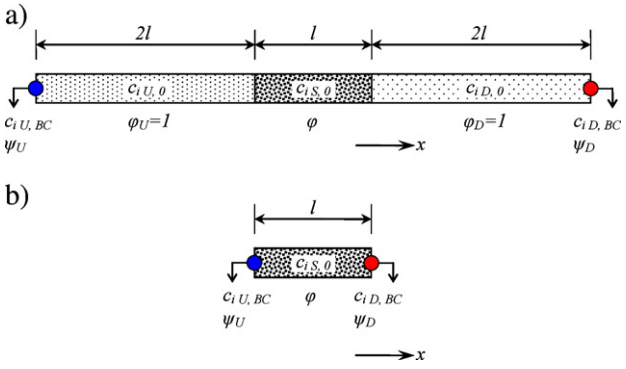

Fig. 3. 1D numerical models: a) three-domain model with initial conditions $c_{i\,U,0}$, $c_{i\,S,0}$ and $c_{i\,D,0}$ for the upstream, specimen and downstream domains (at time $t=0$) and boundary conditions $c_{i\,U,BC}$, $c_{i\,D,BC}$ and ψ_U and ψ_D for concentrations and electrical potentials upstream and downstream respectively. b) One-domain model and its initial and boundary conditions.

(i.e., $x_d > a \cdot D_{Cl} \cdot t$). Alternatively, one can determine D_i numerically from the following more accurate analytical expression [1,7,23]

$$c_i = \frac{c_0}{2} \cdot \left[\operatorname{erfc}\left(\frac{x - a \cdot D_i \cdot t}{2 \cdot \sqrt{D_i \cdot t}} \right) + e^{a \cdot x} \cdot \operatorname{erfc}\left(\frac{x + a \cdot D_i \cdot t}{2 \cdot \sqrt{D_i \cdot t}} \right) \right] \tag{14}$$

An apparent diffusion coefficient can be also computed following the time-lag approach [10]

$$D_i = \frac{2 \cdot x_d^2 \cdot \left(v \coth \frac{v}{2} - 2 \right)}{t_{lag} \cdot v^2} \tag{15}$$

where $v = z_i \cdot q \cdot \Delta\psi / (k \cdot T)$ and $k = 1.380\ 6505 \times 10^{-23}$ J·K^{-1} is the Boltzmann's constant; $q = 1.602\ 176\ 53 \times 10^{-19}$ C is an elementary charge; and t_{lag} is the time lag as defined in Fig. 2. In this approach, migration tests are mathematically converted into natural diffusion tests through the proportionality given by the time lag, and a multiplying factor is adjusted to best fit experimental data.

Table 2 summarizes these methods commonly used for estimating diffusion coefficients from steady-state and non-steady-state migrations tests. Further details of each method can be found in their respective references.

4. Numerical simulations

Eqs. (6) and (7) can be used simultaneously to model the transport of ions under the assumptions previously stated: specimens are saturated and ion transport only occurs within the pore space; advection is not considered; and chemical reactions and activity are neglected. Eqs. (6) and (7) provide a system of $n+1$ differential algebraic equations (i.e., n PDEs and one algebraic equation) for the $n+1$ unknowns (i.e., n concentrations c_i and the electric potential ψ). This system of equations has to be solved simultaneously applying appropriate initial and boundary conditions. The numerical treatment of these equations using the Finite Element Method (FEM) has been discussed in several papers[3] [16,24]. Here we employ the multiphysics package COMSOL to numerically solve these equations using FEM (for more details on the implementation see COMSOL Chemical Engineering Module) [25].

The code is validated against available analytical solutions and experimental data obtained elsewhere. Then the influence of the 'constant field' assumption is quantified. Then chloride diffusion coefficients computed using Eqs. (9)–(15) are compared with the 'true' value, i.e., with the apparent diffusion coefficient used in Eq. (6) to simulate migration tests. Moreover, the effects of the applied voltage difference are presented as well as the influence of using different salt and ionic concentrations in the upstream compartment.

4.1. Finite element model

Migration tests (Fig. 1) are simulated in this work using two different one-dimensional models: a model with three domains, namely the upstream, the specimen and the downstream domains; and a model with one domain representing the specimen of thickness l. Fig. 3-a shows the three-domain model and its boundary conditions. The initial concentrations for each of the ionic species i are specified as initial conditions $c_{i\,U,0}$, $c_{i\,S,0}$ and $c_{i\,D,0}$ for the upstream, specimen and downstream domains (at time $t=0$). Boundary conditions $c_{i\,U,BC}$, $c_{i\,D,BC}$ and ψ_U and ψ_D for concentrations and electrical potentials upstream and downstream are also prescribed. Fig. 3-b shows the one-domain model and its boundary conditions, a model used elsewhere [1,16,20], but incapable of providing transient information of the upstream and downstream compartments. Based on a parametric study on mesh size, time stepping and relative tolerance for both models, optimal values are chosen. As a result, Fig. 3-a is modeled with 264 elements and quadratic shape functions, while Fig. 3-b uses 358 elements; which ensures convergence of results.

The FEM model and the use of Eqs. (6) and (7) are further validated with experimental data from the literature. Two cases are analyzed: Case 1, migration test experimental results on the evolution of current density with time for a concrete specimen with water–cement ratio $w/c=0.5$ [1]; Case 2, experimental results on the evolution of current density with time for mortar specimens with $w/c=0.35$, 0.5 and 0.7 [2].

4.1.1. Case 1

The FEM model uses Eqs. (6) and (7) to approximate experimental data on concrete from the literature [1]. The successive forward simulation technique [26] is used to find the tortuosity τ and initial specimen pore fluid concentrations $c_{i\,S,0}$ that minimize error between the measured and computed electrical current density,

$$\text{Error}_n = \left(\sum_k \left| i_{mes,k} - i_{elec,k} \right|^n \right)^{1/n} \tag{16}$$

[3] It is noted that from the electroneutrality condition generally one concentration can be expressed in terms of the remaining concentrations and be back-substituted into the mass balance equations; hence, reducing the system to n equations with n unknowns.

Table 3
Geometry, initial and boundary conditions

Case 1	$A_s=4.54\cdot10^{-3}$ m^2	$\varphi=0.184$	$\psi_U=0$ V	$\psi_D=10.3$ V	$l=25$ mm
	i	D_{0i} [10^{-9} m^2/s]	$c_{i\ U,0}$ and $c_{i\ U,BC}$ [mol/m^3]	$c_{i\ D,0}$ and $c_{i\ D,BC}$ [mol/m^3]	$c_{i\ S,0}$ [a] [mol/m^3]
	OH^-	5.273	300.0	300.0	1070
	Na^+	1.334	800.0	300.0	1000
	K^+	1.957	0.0	0.0	70
	Cl^-	2.032	500.0	0.0	0
Case 2	A_s=unknown	φ=unknown [a]	$\psi_U=0$ V	$\psi_D=3$ V	$l=10$ mm
	i	D_{0i} [10^{-9} m^2/s]	$c_{i\ U,0}$ and $c_{i\ U,BC}$ [mol/m^3]	$c_{i\ D,0}$ and $c_{i\ D,BC}$ [mol/m^3]	$c_{i\ S,0}$ [a] [mol/m^3]
	OH^-	5.273	108	108	400
	Na^+	1.334	525	25	93
	K^+	1.957	83	83	307
	Cl^-	2.032	500	0	0

Notation: A_s – exposed cross-section area; φ – porosity; l – specimen thickness; ψ_U and ψ_D – electrical potential upstream and downstream; i – ionic species; D_{0i} – self-diffusion coefficient; $c_{i\ U,0}$; $c_{i\ S,0}$ and $c_{i\ D,0}$ – upstream, specimen and downstream initial concentrations (at time $t=0$); $c_{i\ U,BC}$; $c_{i\ D,BC}$ – upstream and downstream concentration boundary conditions. Refer to Fig. 3.

[a] After optimization. Optimized φ are 0.20 ($w/c=0.35$), 0.22 ($w/c=0.5$) and 0.24 $w/c=0.7$) for Case 2.

where i_{mes} is the measured current density and i_{elec} is the electrical current density computed using Eq. (4), at corresponding times k. We use the most common norms, i.e., $n=1$, 2, and ∞. The initial and boundary conditions are specified in Table 3 — Case 1. The apparent diffusion coefficients D_i are then computed with Eq. (2). Fig. 4-a shows the comparison between the experimental data from [1] and the computed current density using the one-domain and the three-domain models (Fig. 3). The evolution of Eq. (16) as a function of OH^- initial concentration within the concrete specimen and tortuosity are shown in Fig. 4-b and -c respectively.[4] The chloride apparent diffusion coefficient corresponding to the best approximation is $D_{Cl}=6.17\times10^{-12}$ m^2 s^{-1}.

4.1.2. Case 2

Again, Eqs. (6) and (7) are used to approximate experimental data on mortars from the literature [2]. The initial and boundary conditions are specified in Table 3 — Case 2. Since mortar porosity is not reported, porosity is another optimization parameter along with tortuosity, OH^-, Na^+ and K^+ initial specimen pore fluid concentrations $c_{i\ S,0}$. The set of values that minimize the error (Eq. (16)) is found by successive forward simulation. A summary of the numerical results is shown in Fig. 4-d. Fig. 4-b and -c illustrate the L_2 norm error minimization as a function of tortuosity and of OH^- initial specimen pore fluid concentration.

In Case 2, experimental fluxes are also reported [2] and in good agreement with the computed fluxes: the experimentally measured chloride fluxes are 1.35×10^{-5} mol (m^2 s)$^{-1}$ for $w/c=0.35$, 1.81×10^{-5} mol (m^2 s)$^{-1}$ for $w/c=0.5$, and 3.35×10^{-5} mol (m^2 s)$^{-1}$ for $w/c=0.7$; and the numerically computed fluxes are 1.3×10^{-5} mol (m^2 s)$^{-1}$, 2.3×10^{-5} mol (m^2 s)$^{-1}$, and 3.3×10^{-5} mol (m^2 s)$^{-1}$ respectively. The chloride apparent diffusion coefficient corresponding to the best approximations are $D_{Cl}=7.88\times10^{-12}$ m^2 s^{-1}; $D_{Cl}=9.83\times10^{-12}$ m^2 s^{-1}; and $D_{Cl}=12.7\times10^{-12}$ m^2 s^{-1} for $w/c=0.35$; 0.5 and 0.7 correspondingly.

4.2. Influence of main parameters

Eqs. (9)–(15) are used to compute apparent diffusion coefficients. These equations are presented as a result of simplifications of the governing equations (see Section 3). In this section, we take a close look of the transport of ions through cement-based specimens. We consider that experiments are conducted in isothermal conditions and therefore, the effect of temperature is not shown.

4.2.1. Pore fluid composition/ion species

The pore fluid composition of concrete specimens is rarely reported in migration tests, in part due to the difficulties on obtaining accurate results. Although the initial pore fluid composition is usually assumed to be same as for the curing specimen environment, the successive forward simulations reveal that the pore fluid composition is, in general, different. We take Case 1 (Section 4.1.1), and we monitor the ionic concentration variations in time within the specimen (Fig. 5). It is observed that there is indeed cation migration (Na^+, K^+) towards the cathodic compartment and anion movement (OH^- and Cl^-) towards the anodic compartment (compare with Fig. 1). More importantly, ions that are not initially present in the upstream or downstream compartments (i.e., K^+) migrate out of the specimen within ~30 h; while the excess concentration of other ions (i.e., concentration difference on top of upstream and downstream compartments concentrations) transport out in ~10 h and continue their migration thereafter (OH^- and Na^+).

4.2.2. Electric potential

It is usually assumed that the electric potential varies linearly within the specimen. Fig. 6-a shows the variation of the potential

[4] We verified that small initial specimen concentrations of other ions such as SO_4^{2-} and Ca^{2+} do not significantly affect the overall current density, and are not included here for clarity.

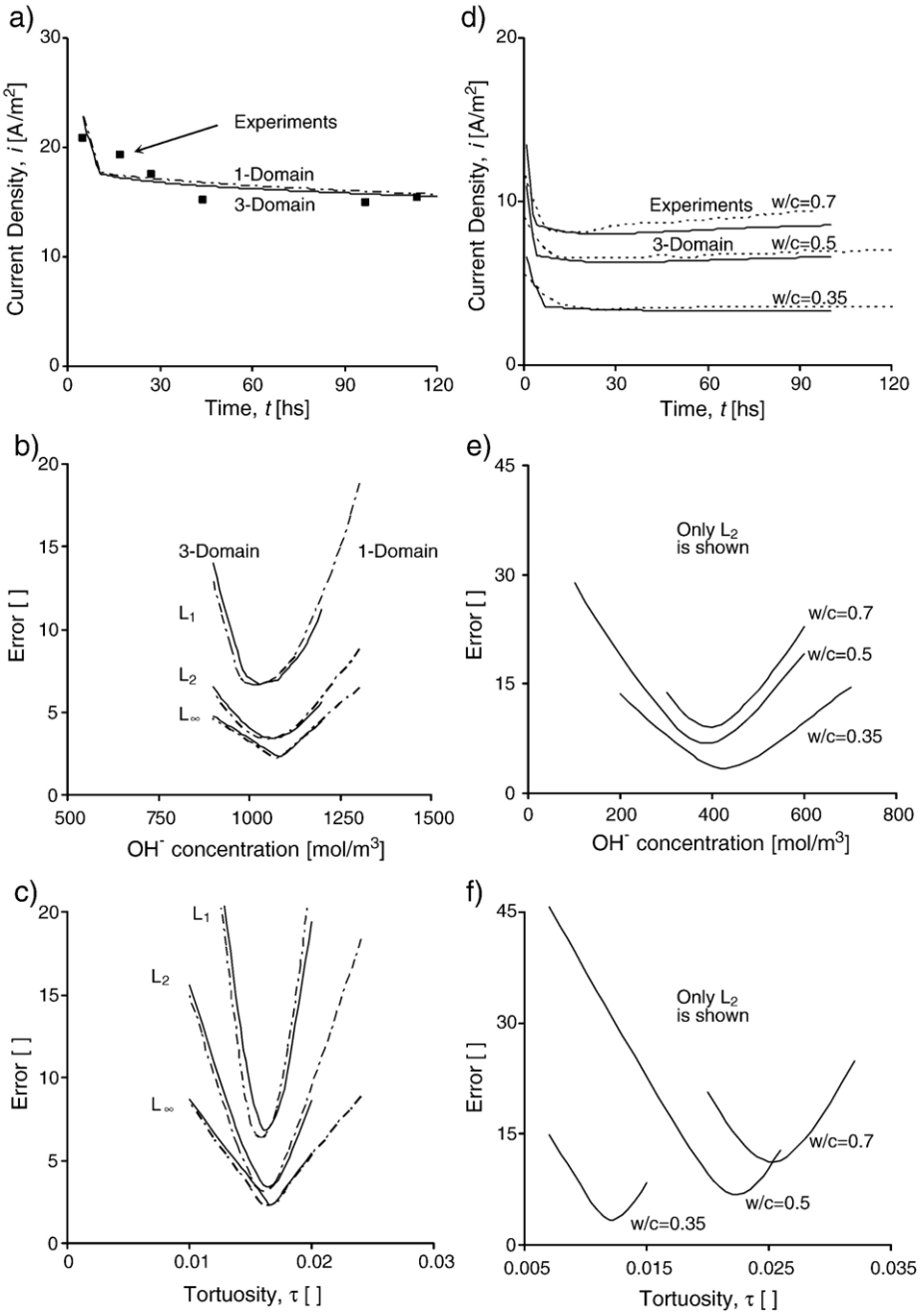

Fig. 4. Validation of the finite element model: a) Case 1, comparison between experimental data from [1] and the computed current density using the one-domain and the three-domain models (Fig. 3). b) Error minimization (Eq. (16)) as a function of the OH^- specimen initial concentration and c) tortuosity (L_1, L_2 and L_∞ are shown). d) Case 2, comparison between experimental data from [2] (doted line) and numerical results (solid line) using three-domain models. e) and f) Error minimization for Case 2 (only L_2 norm are shown).

with specimen depth for Case 1, similar results are obtained for Case 2. Fig. 6-a clearly indicates that the electric potential is generally not linear.

The electric field can be computed as:

$$E = -\frac{\partial \psi}{\partial x} \tag{17}$$

where ψ is the electric potential or voltage. A linearly varying potential means a constant electric field. It is observed that the electric field is not constant at any time during the migration test, in particular before ~20 h (Fig. 6-b). Nevertheless, it becomes more stable thereafter. Even though the electric field is constant between 1/4 and 3/4 of the total specimen thickness at times greater than ~20 h, the constant field in this region is approximately 8% lower than the expected external field E_{ext},

$$E_{ext} = -\frac{\Delta \psi}{l} \tag{18}$$

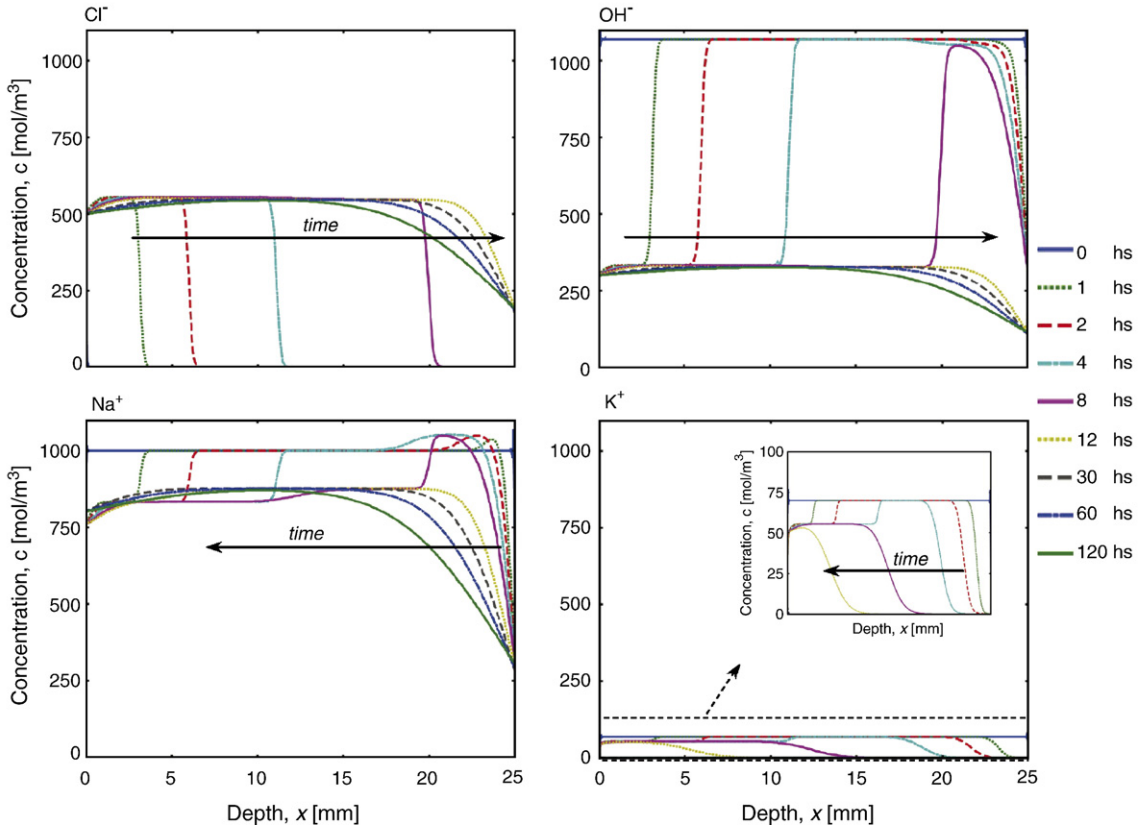

Fig. 5. Pore fluid composition and the time-varying concentration of ions within the specimen (Case 1 is shown).

where ψ is the electric potential or voltage (in this case, E_{ext}= 412 V m^{-1}). Moreover, the electric field in the specimen is up to 2.5 times higher closer to the downstream compartment.

4.2.3. Ionic concentrations upstream

The added salt concentration in the upstream compartment is varied and its effects on the electrical potential ψ across the cement-based specimen are computed.

Consider the three-domain-model for Case 1 (Table 3 — Case 1) but with salt concentrations ranging from 0.0125 M through 1.5 M, with corresponding boundary and initial conditions (as in Table 1). Eqs. (6) and (7) are simultaneously solved using COMSOL for each of these initial and boundary conditions. Fig. 7-a summarizes the effects on the voltage within the specimen. As the upstream NaCl concentration increases, voltage non-linearity increases. Fig. 7-b shows the effects of increasing upstream salt concentration on the current density transient response. The time lag decreases with increasing salt concentration. However, the steady-state current density only slightly varies by 6% for the whole range of concentrations, with a tendency to increase.

4.2.4. External voltage

The effects of applied external voltage on migrations tests are also explored using the three-domain-model for Case 1. Fig. 8-a shows the influence of the applied external voltage on current density over time. It is shown that current density increases with increasing applied voltage. In addition, steady-state is reached faster. The combined effects of both externally applied voltage difference and varying salt concentration in the upstream compartment can be seen in Fig. 8-b. The non-linearity of the electrical field increases as both parameters augment.

5. Analysis and discussion

The pore fluid composition of cement-based specimens is usually not reported, due to the difficulties on obtaining accurate results, and the initial pore fluid composition is typically assumed to be same as for the curing specimen environment. However, the successive forward simulations performed in this work shows that the pore fluid within the specimen may be different from the curing solution as a result of chemical reactions throughout curing (some experimental evidence is also available [1,2]). Nevertheless, the differences seen here do not greatly affect pH levels (e.g., from pH = 13.7 to pH = 14 in Case 1); thus they may not be easily detected before the migration test starts. Furthermore, excess ions migrate out of the specimen and delay chloride migration, while its apparent diffusion coefficient is lowered. Although the estimation of the average apparent diffusion coefficient is not greatly affected by the specimen initial pore solution, the overall current density versus time response is influenced significantly. A total of four experimental data sets are analyzed in this work; however, more comparisons with data where pore solution after curing is measured are needed.

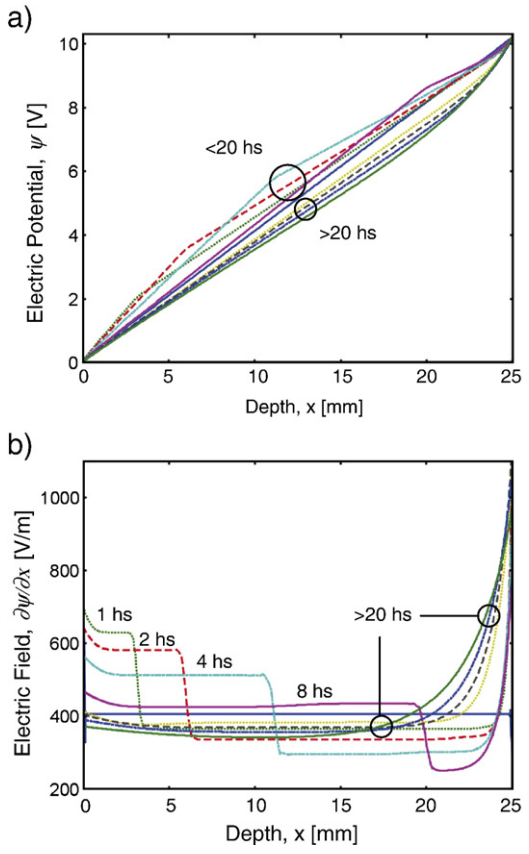

Fig. 6. Electric potential (Case 1 is shown): a) non-linear variation of electrical potential with depth, b) variation of electrical field with depth.

Most of the simplified expressions for estimating diffusion coefficients are a function of ionic flux density and concentrations. Fig. 9-a shows as an example the chloride flux density evolution with time throughout the specimen. Due to the variation of concentrations with time within the specimen (Fig. 5), one may wonder if the flux density is constant within the sample at steady-state.

Fig. 9-b shows that indeed the flux tends to be constant. Moreover, the dominant driving force can be estimated from the ratio between the migration and diffusive components of the flux (Eq. (3)). The migration component certainly dominates in migration tests, with increasing importance up to the time lag, where it is 600 times larger than the diffusive component (Case 1 — Fig. 10). Therefore, neglecting the diffusive component as in Eqs. (9)–(12) in steady-state migration tests is reasonable for practical purposes.

Nevertheless, Eqs. (9)–(12) also assume a constant electric field. In addition, the location x where the input parameter concentration is taken may lead to inaccuracies for both non-steady and steady-state tests. Fig. 11 shows a summary of chloride diffusion coefficient estimations using formulae in Table 2 for a salt concentration range upstream from 0.012 M through 1.5 M and external applied voltage difference ranging between 3 V and 18 V, in a specimen of 25 mm thickness.[5]

[5] Results from Eqs. (13) and (14) are not looked at due to their inadequacy to capture chloride profiles as of Fig. 5.

Theoretical 'true' apparent chloride diffusion coefficient obtained from solving the Nernst–Planck equations coupled with the electroneutrality condition are also shown (see dashed line in Fig. 11). Chloride concentrations in these computations are taken in the upstream compartment c_U, downstream compartment c_D, at the midpoint within the specimen $c_{Midpoint}$ and as an average value $c_{average}$.

Eqs. (9) and (11) deliver the same result in consequence of the relationship that exists between flux density and current density given by Eq. (4). Therefore, we recommend the monitoring of both, concentration (i.e., flux) and current density during testing. We believe that the use of more than one measurement would become a good practice to minimize experimental errors since both parameters (flux and current density) should deliver the same chloride diffusion coefficient. Our numerical simulations in Fig. 11-a show slight tendency of decreasing diffusion coefficient with increasing salt concentration in the upstream compartment, also observed in experiments [10] when employing Eq. (9).

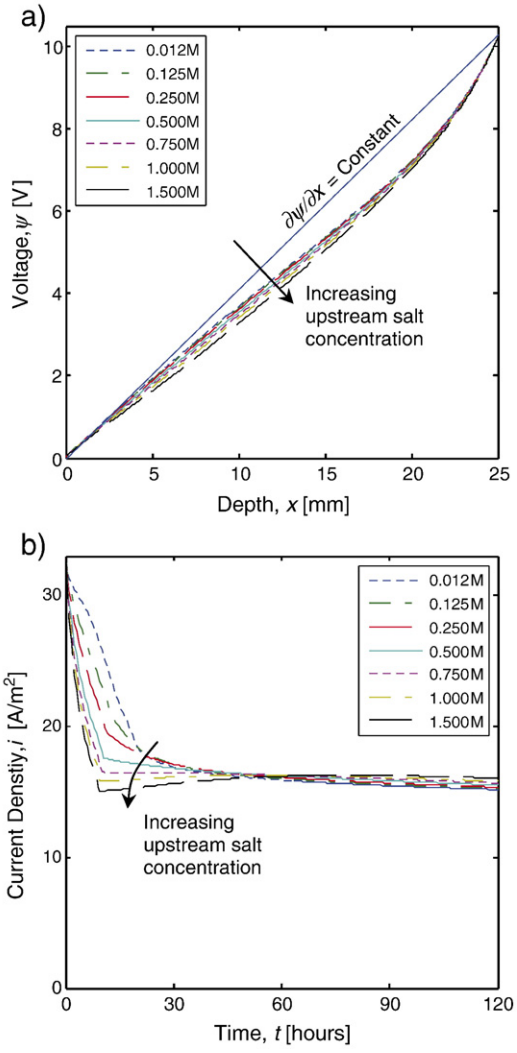

Fig. 7. Influence of ionic upstream concentration (based on Case 1): a) voltage within the specimen with varying NaCl concentration in upstream compartment. b) Current density perturbation.

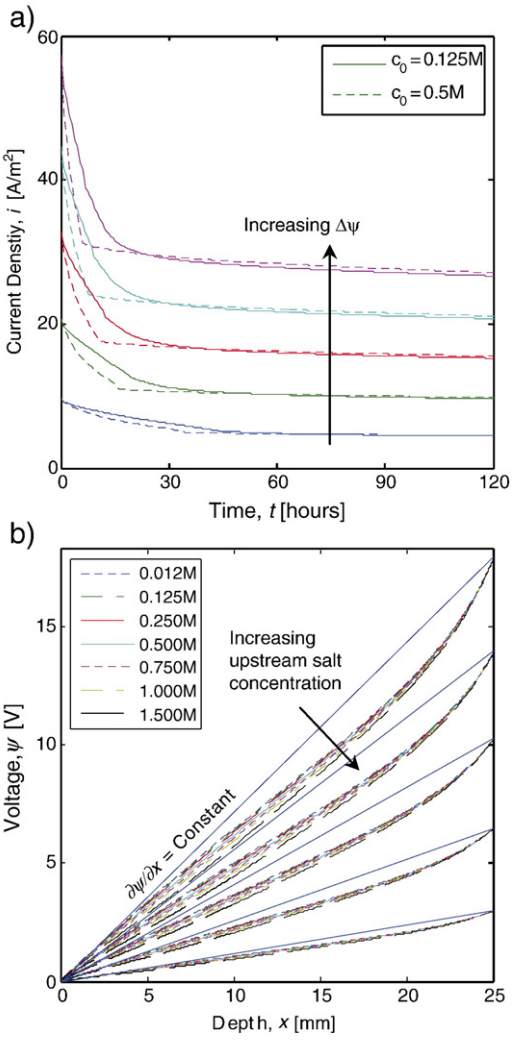

Fig. 8. Influence of applied external voltage difference (based on Case 1): a) current density variation over time as function of external voltage. b) Voltage within the specimen with varying NaCl concentration in upstream compartment.

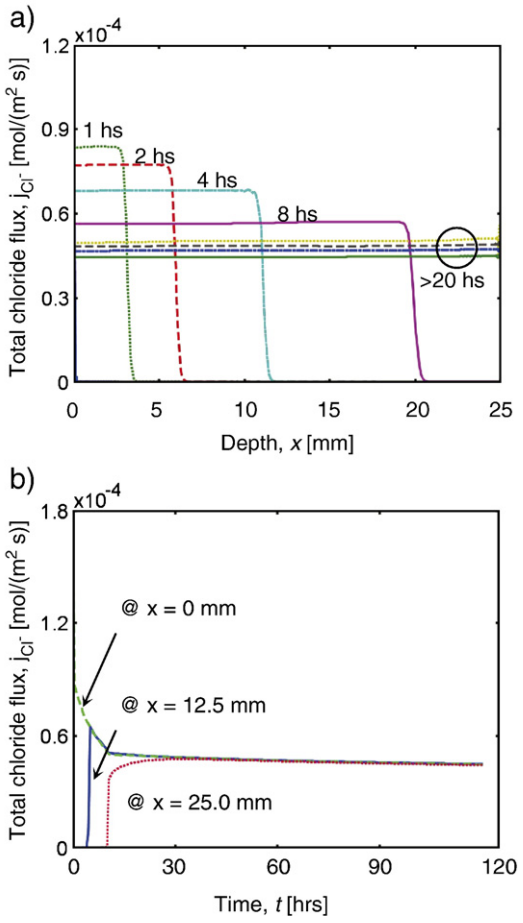

Fig. 9. Chloride flux density (Case 1 is shown): a) its variation with depth within the specimen. b) Cl^- flux density variation with time.

The use of Eq. (10) yields the same chloride diffusion coefficients as of Eqs. (9) and (11) when the chloride concentration is taken in the downstream compartment c_D and is strongly affected by the external electric field, decreasing as the external voltage difference increases (Fig. 11-a). Practitioners should avoid making the mistake of considering c_D in the estimation of Cl^- diffusion coefficient.

Eq. (15) does not give accurate results; it shows dependency of the source salt concentration and of the external electric field. Although the determination of x_d from our numerical simulations is challenging, we show in Fig. 11-b the outcome of using x_d as one third of the total specimen thickness. This represents the best realistic scenario, since the use of larger x_d would render even higher chloride diffusion coefficients.

Fig. 11-b reveals that the use of measured average upstream concentrations c_U, as a practical substitute of the difficult-to-obtained specimen average concentration $c_{Average}$, gives results with less than 10% difference in the estimation of diffusion coefficients between them. Moreover, Eqs. (9) and (11) with employment of upstream concentrations yield a chloride diffusion coefficient only 10% lower than the 'true' apparent diffusion coefficient employed in the simulation with $c_0 = 500\ mol \cdot m^{-3}$ and $\Delta\psi = 10.3$ V (equivalent to Case 1, Section 4.1.1). This difference is partially justified by the decrease in the actual 'constant' electric field applied to most of the specimen (Section 4.2.2, Fig. 6-b). If instead of the upstream or average concentration, the

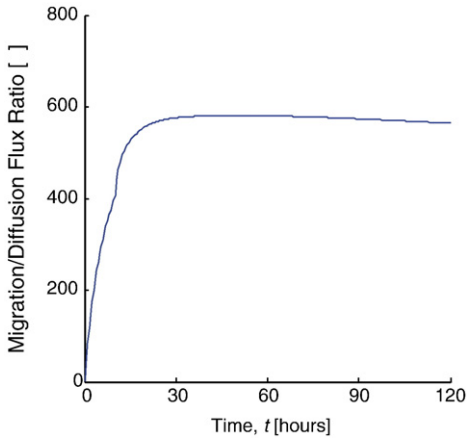

Fig. 10. Dominant driving force in migration tests (Case 1 is shown).

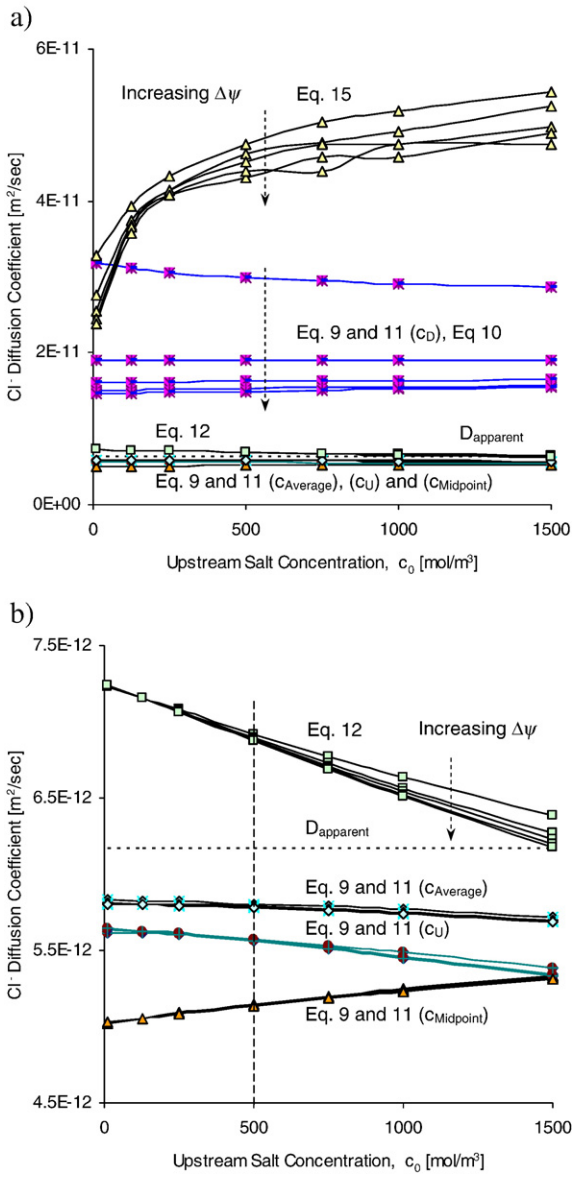

Fig. 11. Chloride diffusion coefficient comparison: a) estimations for varying upstream salt concentration and varying applied external voltage. b) Enlarged view on best estimations.

concentration of the specimen middle point c_{Midpoint} is taken into consideration in Eqs. (9) and (11), then the difference between coefficients estimated with these formulae and the actual apparent coefficient will increase (Fig. 11-b). This is because chloride ions do not transport within the specimen independently of other ions since electroneutrality (Eq. (7)) must be satisfied. Fig. 5 exemplifies such assessment. The electric field makes anions move towards the downstream or anodic compartment; meanwhile cation Na^+ moves in the opposite direction towards the upstream or cathodic compartment against the Na^+ concentration gradient since the migration term overwhelms the diffusive term (Fig. 10).

On the other hand, there is a small ~0.3% variation on the estimation of chloride diffusion coefficient for a large range of externally applied voltage. However, larger voltage differences (i.e., larger electric fields) may induce joule effects [6] and thus it may change the isothermal assumption of this work.

The use of Eq. (12) overestimates the apparent chloride diffusion coefficient by 9% for $c_0 = 500$ mol m^{-3} and $\Delta\psi = 10.3$ V. Diffusion coefficients estimated with this equation tend to decrease as the source salt concentration increases (a 16% variation for the range explored), and also slightly decreases for increasing externally applied voltage show a tendency.

6. Conclusions

Ionic diffusion coefficients can be determined rapidly using electromigration tests. They are accurately simulated here using Nernst–Planck equation coupled with the electroneutrality condition. The following conclusions are drawn:

- Migration due to the external voltage difference overwhelms diffusion due to concentration gradients and chloride ions interact with other ions while migrating since electroneutrality must be satisfied.
- The electric field within the specimen is not constant, although it reaches asymptotic values close to the assumed constant electric field. This difference is of the same order of the error encountered in the estimation of the chloride diffusion coefficient when employing the upstream chloride concentration in Eqs. (9) and (11).
- The variation of external voltage differences strongly affects the current density measured during testing.
- The variation of source chloride concentration induces increasing non-linearity in electrical potential within specimen and modifies the time lag for reaching steady-state condition. It also strongly affects the estimation of diffusion coefficients in non-steady-state tests; however, it does not have such effect in steady-state results.
- The simultaneous use and monitoring of current density and fluxes are recommended for both the non-steady and steady-state migration tests.
- Pore fluid within the specimen may differ from the curing solution, but more experimental data are needed to further verify this observation. The impact of possible changes in the pore solution is minor for changes in pH. The excess ions migrate out of the specimen and delay chloride transport, while its apparent diffusion coefficient is lowered.

Acknowledgements

We thank Reviewer No. 2 for valuable observations. The research is supported by the Australian Research Council, Discovery Grant Project No. DP 50193.

Appendix A

Notation

A_s	specimen cross-section
c_0	initial source concentration (upstream salt concentration)
c_{Average}	average specimen chloride concentration
c_D	downstream average ionic concentrations

c_d ionic concentration at x_d
$c_{i\ D,0}$ initial downstream average pore fluid concentrations of ith ion
$c_{i\ S,0}$ initial specimen average pore fluid concentrations of ith ion
$c_{i\ U,0}$ initial upstream average pore fluid concentrations of ith ion
$c_{i\ U,BC}$; $c_{i\ D,BC}$ upstream and downstream boundary conditions, respectively
c_i average concentration of the ith ion in the fluid phase
$c_{Midpoint}$ chloride concentration at specimen middle point
c_U upstream average ionic concentrations
D_{0Cl} chloride self-diffusion coefficient
D_{0OH} hydroxyl self-diffusion coefficient
D_{0i} self-diffusion coefficient of the ith ion
D_i apparent ion diffusion coefficient of the ith ion.
F Faraday constant = 96,485.3 C mol^{-1}
i_0 initial current density
i_{elec} computed current density
i_f final current density
i_{mes} measured current density
j_i ith ion molar flux density
k Boltzmann's constant = $1.380\ 6505 \times 10^{-23}$ J K^{-1}
l specimen thickness
n_i molar increment of the ith ion
q elementary charge = $1.602\ 176\ 53 \times 10^{-19}$ C
R gas constant = 8.3144 J mol^{-1} K^{-1}
T absolute temperature
t time
t_{lag} time-lag
tr_i transference number of the ionic species
V_x average velocity of the fluid
w/c water–cement ratio
x_d penetration depth
z_i ith ion charge
γ_i chemical activity coefficient of the ith ion
ν time-lag constant = $z_i \cdot q \cdot \Delta\psi/(k \cdot T)$
τ tortuosity
φ porosity
ψ voltage
ψ_U and ψ_D boundary condition in upstream and downstream electrical potentials

References

[1] E. Samson, J. Marchand, K.A. Snyder, Calculation of ionic diffusion coefficients on the basis of migration test results, Materials and Structures/Matériaux et Constructions 36 (257) (2003) 156–165.
[2] H. Friedmann, O. Amiri, A. Aït-Mokhtar, A direct method for determining chloride diffusion coefficient by using migration test, Cement and Concrete Research 34 (11) (2004) 1967–1973.
[3] C.L. Page, K.W.J. Treadaway, Aspects of the electrochemistry of steel in concrete, Nature 297 (5) (1982) 109–115.
[4] P. Pivonka, C. Hellmich, D. Smith, Microscopic effects on chloride diffusivity of cement pastes — a scale-transition analysis, Cement and Concrete Research 34 (12) (2004) 2251–2260.
[5] K.D. Stanish, R.D. Hooton, M.D.A. Thomas, Testing the chloride penetration resistance of concrete: a literature review, FHWA Contract DTFH61-97-R-00022, University of Toronto, Toronto, Ontario, Canada, vol. 2006, June 2000.
[6] C. Andrade, Calculation of chloride diffusion coefficients in concrete from ionic migration measurements, Cement and Concrete Research 23 (3) (1993) 724–742.
[7] L. Tang, Electrically accelerated methods for determining chloride diffusivity in concrete — current development, Magazine of Concrete Research 48 (176) (1996) 173–179.
[8] A. Delagrave, J. Marchand, E. Samson, Prediction of diffusion coefficients in cement-based materials on the basis of migration experiments, Cement and Concrete Research 26 (12) (1996) 1831–1842.
[9] C. Andrade, M. Castellote, C. Alonso, C. Gonzalez, Non-steady-state chloride diffusion coefficients obtained from migration and natural diffusion tests. Part I: Comparison between several methods of calculation, Materials and Structures/Matériaux et Constructions 33 (225) (2000) 21–28.
[10] M. Castellote, C. Andrade, C. Alonso, Measurement of the steady and non-steady-state chloride diffusion coefficients in a migration test by means of monitoring the conductivity in the anolyte chamber. Comparison with natural diffusion tests, Cement and Concrete Research 31 (10) (2001) 1411–1420.
[11] T. Zhang, O.E. Gjørv, Effect of ionic interaction in migration testing of chloride diffusivity in concrete, Cement and Concrete Research 25 (7) (1995) 1535–1542.
[12] P.F. McGrath, R.D. Hooton, Influence of voltage on chloride diffusion coefficients from chloride migration tests, Cement and Concrete Research 26 (8) (1996) 1239–1244.
[13] T. Zhang, O.E. Gjørv, Effect of chloride source concentration on chloride diffusivity in concrete, ACI Material Journal 102 (5) (2005) 295–298.
[14] F.G. Helfferich, Ion Exchange, McGraw-Hill, New York, 1962, p. 624.
[15] R. Barbarulo, J. Marchand, K.A. Snyder, S. Prene, Dimensional analysis of ionic transport problems in hydrated cement systems: Part 1. Theoretical considerations, Cement and Concrete Research 30 (12) (2000) 1955–1960.
[16] E. Samson, J. Marchand, Numerical solution of the extended Nernst–Planck model, Journal of Colloid and Interface Science 215 (1999) 1–8.
[17] J. Arsenault, Etude des mécanismes de transport des ions chlore dans le béton en vue de la mise au point d'un essai de migration, INSA Génie civil, Toulouse, France et Faculté des sciences et de génie, Laval, Québec, 1999.
[18] J. Bear, Y. Bachmat, Introduction to Modelling of Transport Phenomena in Porous Media, Kluwer Academic Publishers, Dordrecht, The Netherlands, 1991.
[19] D. Smith, P. Pivonka, C. Jungnickel, S. Fityus, Theoretical analysis of anion exclusion and diffusive transport through platy-clay soils, Transport in Porous Media 57 (3) (2004) 251–277.
[20] O. Truc, J.-P. Ollivier, L.-O. Nilsson, Numerical simulation of multi-species transport through saturated concrete during a migration test — MsDiff code, Cement and Concrete Research 30 (10) (2000) 1581–1592.
[21] A.D. MacGillivray, Nernst-Planck equations and the electroneutrality and Donnan equilibrium assumptions, Journal of Chemical Physics 48 (1968) 2903–2907.
[22] M. Kato, Numerical analysis of the Nernst–Planck–Poisson system, Journal of Theoretical Biology 177 (3) (1995) 299–304.
[23] L. Tang, L.-O. Nilsson, Rapid determination of chloride diffusivity of concrete by applying an electric field, ACI Material Journal 89 (1) (1992) 49–53.
[24] K. Kabbenhoft, P. Pivonka, S.W. Sloan, D. Smith, Numerical aspects of multiionic transport in electrolytic solutions, in: Y. Abousleiman, A. Cheng, F.-J. Ulm (Eds.), Proceedings of the 3rd Biot Conference on Poromechanis, A.A. Balkema Publishers, London, UK, 2005, pp. 411–416.
[25] I. Comsol AB, COMSOL Multiphysics: Chemical Engineering Module User's Guide, Stockholm, Sweden, 2005, p. 348.
[26] J.C. Santamarina, D. Fratta, Discrete Signals and Inverse Problems — An Introduction to Engineers and Scientists, John Wiley & Sons, Hoboken, NJ, 2005, p. 364.